JSTR
ASEAN Journal of Scientific and Technological Reports

Research article

Preparation of Lead-Free X-Ray Shielding Materials Based on Natural Rubber/Barium Sulfate Composites

Sutthisa Konruang[1]* Arnon Srisook[2] Pornpana Buaphet[3] Fadeelah Tayeh[4] Weerawut Naebpetch[5]

[1] Department of Physics, Faculty of Science, Thaksin University, Phatthalung, 93210, Thailand; sutthisa@tsu.ac.th.
[2] Regional Medical Sciences Center 11 Suratthani, Surat Thani, 84100, Thailand; arnon.s@dmsc.mail.go.th.
[3] Department of Physics, Faculty of Science, Thaksin University, Phatthalung, 93210, Thailand; pornpana@tsu.ac.th.
[4] Department of Physics, Faculty of Science, Thaksin University, Phatthalung, 93210, Thailand; 612021200@tsu.ac.th.
[5] Center of rubber technology for community, Faculty of Engineering, Thaksin University, Phatthalung, 93210, Thailand; Berm_lif@hotmail.com.
* Correspondence: e-mail ; sutthisa@tsu.ac.th

Citation:
Konruang, S.; Srisook, A.; Buaphet, P.; Tayeh, F.; Naebpetch, W. Preparation of Lead-Free X-Ray Shielding Materials Based on Natural Rubber/Barium Sulfate Composites. *ASEAN J. Sci. Tech. Report.* **2022**, *25(2)*, 59-66. https://doi.org/10.55164/ajstr.v25i2.246574.

Article history:
Received: May 2, 2021
Revised: June 24, 2022
Accepted: June 24, 2022
Available online: June 26, 2022

Abstract: This work prepared the lead-free X-ray shielding materials based on natural rubber (NR) mixed with $BaSO_4$ particles at different $BaSO_4$ contents (0–100 phr) and different material thicknesses (0.5-2.5 cm). The X-ray shielding properties of NR/$BaSO_4$ composites were tested using a 100-kV X-ray generator. The results suggested that the increases in the $BaSO_4$ contents improved the x-ray shielding properties of the NR/$BaSO_4$ composites, such as linear attenuation coefficient (μ_l), mass attenuation coefficient (μ_m), and half-value layer (HVL). The highest X-ray attenuation was 94 % in 100 phr $BaSO_4$. In terms of mechanical properties, it was found that the density and hardness (Shore A) increased with increasing $BaSO_4$ contents. In contrast, the increases in $BaSO_4$ resulted in decreased tensile strength, elongation at break and tear strength. In summary, the overall properties suggest that these NR/ $BaSO_4$ composites could be developed as an effective X-ray shielding material instead of lead.

Keywords: Natural rubber; Barium sulfate; X-ray shielding; Composite materials

1. Introduction

X-ray is a relatively high-energy electromagnetic wave that plays important roles in various applications such as agriculture, food preservation, industry, and especially in medical fields for diagnosis and therapy [1]. However, exposure to X-rays could potentially lead to fatal health hazards in radiation workers and users and cause symptoms such as skin burns and vomiting within hours. It can also result in long-term health effects such as memory loss, cancer, and cardiovascular disease [2]. Therefore, effective shielding materials were important to prevent excessive X-ray exposure. It is known that the materials composed of high-atomic-number (Z) and high-density elements are commonly used as shielding materials, such as lead (Pb) [3-5].

However, lead is considered a hazardous chemical [6]. Recently, the radiation shielding materials with the addition of fillers such as tungsten oxide (W_2O_3) [7-8], bismuth oxide (Bi_2O_3) [8-10], and barium sulfate ($BaSO_4$) [7,11-12] were studied for replacement of lead (Pb). Among these materials, $BaSO_4$ is an exciting filler since it is environmentally friendly, safe, and highly effective in X-ray attenuation [12]. Previous investigations reported that it could be improved the radiation shielding properties of concrete [13] and it is also found that a shielding film prepared from $BaSO_4$ and polymeric silicon has higher tensile strength and X-ray shielding performance [7]. In addition, a polymeric composition consisting of ethylene propylene diene monomer (EPDM), industrial oil (IO), and alkyl phenol-formaldehyde resin (PF) with the addition of $BaSO_4$ can be applied to manufactured material for protection from radiation in offices of radiation therapy and diagnostics [12].

In this work, we aimed to develop flexible and lead-free X-ray-shielding materials that are safe and environmental-friendly based on NR/$BaSO_4$ composites. Dunlop method is used for NR/$BaSO_4$ composites foam production. This method is widely used because it is simple, convenient, reliable, cost-effective, and energy-efficient [14-15]. The X-Ray shielding properties are tested based on the thicknesses and $BaSO_4$ contents of NR/$BaSO_4$ composites, such as X-ray transmission ratio, X-ray attenuation, linear attenuation coefficient (μ_l), mass attenuation coefficient (μ_m), and half-value layer (HVL). Furthermore, the mechanical properties of the composites were also investigated.

2. Materials and Methods

1. Materials

NR latex with 60 wt% dry rubber was acquired from the Center of rubber technology for community, Faculty of engineering, Thaksin University, Phatthalung, Thailand. Barium Sulfate was purchased from Scitrader Co, Ltd. (Thailand). Sulfur (S), zinc diethyldithiocarbamate (ZDEC), zinc 2-mercaptobenzothiazole (ZMBT), Wingstay®-L, zinc oxide (ZnO), Diphenylguanidine (DPG), and Sodium silicofluoride (SSF) was purchased from VPK Supply Co, Ltd. (Thailand). All chemicals were used in an aqueous dispersion form, prepared in the laboratory (Table 1).

2. Preparation of NR/$BaSO_4$ composites

NR/$BaSO_4$ composites were fabricated using the chemical proportions given in Table 1. First, NR latex was filtered and agitated by a whisk and bowl mixer for 3 min to liberate dissolved ammonia before foam preparation. After that, $BaSO_4$, S, ZDEC, ZMBT, Wingstay® L, ZnO, DPG and SSF were slowly added to the mixture and stirred for about 1 min. Then, the NR/$BaSO_4$ foam was poured into a mold (25x25x0.5 cm^3) to begin the gelling process. Finally, NR/$BaSO_4$ was vulcanized at 100 ◦C for 1 h in an oven (ED 56, BINDER). The non-reactive reagents were removed by washing the solid foam with distilled water. After washing, the cured NR/$BaSO_4$ was evenly dried in a hot air oven at 80°C for 24 h.

Table 1. Material formulations for Natural Rubber/Barium Sulfate Composites preparation

Ingredients	Total solid content (%)	Dry weight (phr*)	Wet weight (g)
HA latex	60	100	167
S	50	2	4
ZDEC	50	2.5	5
ZMBT	50	2	4
Wingstay® L	50	1	2
ZnO	50	5	10
DPG	40	2	5
SSF	20	0.5	2.5
$BaSO_4$ (phr)	0, 50, 75, 100		

* phr is the ratio unit of weight part of chemicals to 100 wt parts of rubber

3. Characterizations

3.1. Density and morphology studies

For all NR/$BaSO_4$ composites, the density was measured by comparative measurement of each sample mass in air and water using a digital scale (BSA Series, Sartorius). The experimental setup showed in Figure 1. The samples with dimensions of 20 × 20 × 5 mm^3 were placed in the balance pan and recorded their dry weight. Next, the samples were placed under the submersed basket. Finally, the specific gravity was calculated by a digital scale. The specific gravity of the sample was multiplied by water density to obtain the density of the sample, as shown in Eq (1).

$$specific\ gravity = \frac{density\ of\ the\ object}{density\ of\ the\ water} \tag{1}$$

For the study of morphology, the samples were investigated using a scanning electron microscope (SEM; FEI / FEG Quanta 450), operating at 5 kV. Dried foams were vacuum-coated with gold before SEM investigation.

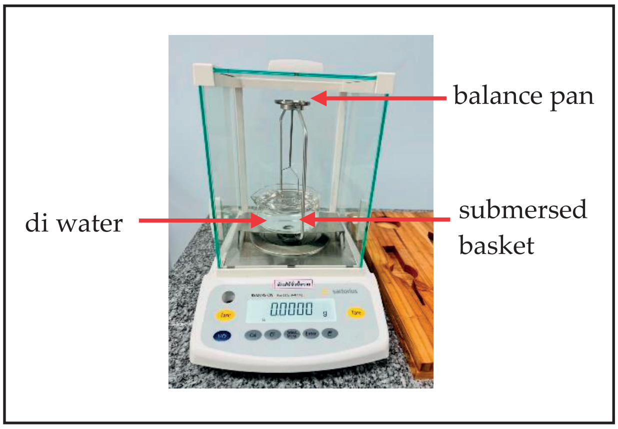

Figure 1. Setup for Density measurement.

2.2. Mechanical properties

Tensile and tear tests were conducted following ISO37-1 and ISO30-1, respectively, to characterize the mechanical properties of the NR/$BaSO_4$ composites. The tests were performed on a universal testing machine (Purchem Co., Ltd.) with a crosshead speed of 50 cm/min. Ultimate tensile strength, elongation at break and tear strength were determined. The hardness for all NR/$BaSO_4$ was tested using an automatic hardness tester (GX-02, Teclock).

2.3. X-Ray shielding properties

The X-Ray shielding properties of NR/$BaSO_4$ composites were performed at the Chaiya Hospital, Surat Thani Province, using the General X-ray Machine (MRAD-A32S, CANON) at 100 kV and the X-ray test equipment (X2, RAYSAFE) was used as the detector. All samples used in the experiment were 2 cm × 2 cm. The X-Ray shielding properties test was carried out on the different material thicknesses (0.5-2.5 cm). The narrow beam X-ray source was located 1 m from the surface of NR/$BaSO_4$ composites. The independent 0.05 s tests were performed and were recorded for each sample. The experimental setup is shown in Figure 2. From the experiment, the X-Ray shielding properties included X-ray attenuation [2], linear attenuation coefficient (μ_l), mass attenuation coefficient (μ_m), and half-value layer (HVL) [7] could be calculated using equation (2) – (5)

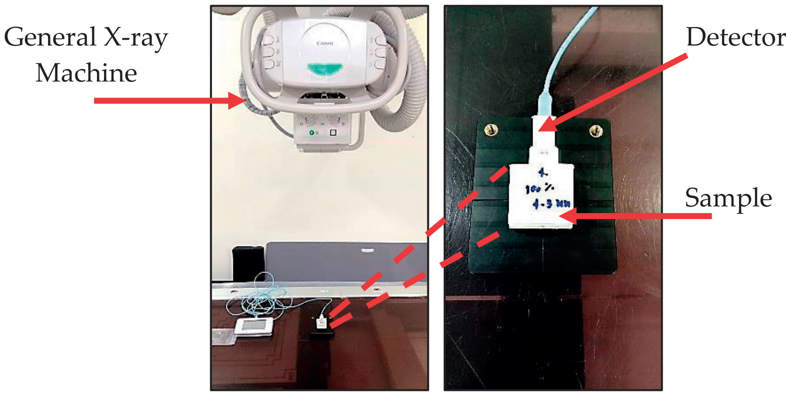

Figure 2. Setup for X-ray shielding measurement.

$$X - ray\ attenuation = \frac{I_0 - I}{I_0} \times 100 \quad (2)$$

$$I = I_0 e^{-\mu_l x} \quad (3)$$

$$\mu_m = \frac{\mu_l}{\rho} \quad (4)$$

$$HVL = \frac{ln\,2}{\mu_l} \quad (5)$$

Where I, I_0, μ_l, μ_m, ρ, HVL, and x was the intensity of transmitted X-rays, the intensity of incident X-rays, linear attenuation coefficient, mass attenuation coefficient, density, half-value layer, and thickness of the samples, respectively.

3. Results and Discussion

3.1 Density and morphology studies

The density of NR/$BaSO_4$ composites is shown in Figure 3. It was found that the densities of NR/$BaSO_4$ composites increased with $BaSO_4$ content mainly due to the much higher density of $BaSO_4$ particles. It was known that increased material density could improve the mass attenuation coefficient according to equation 4.

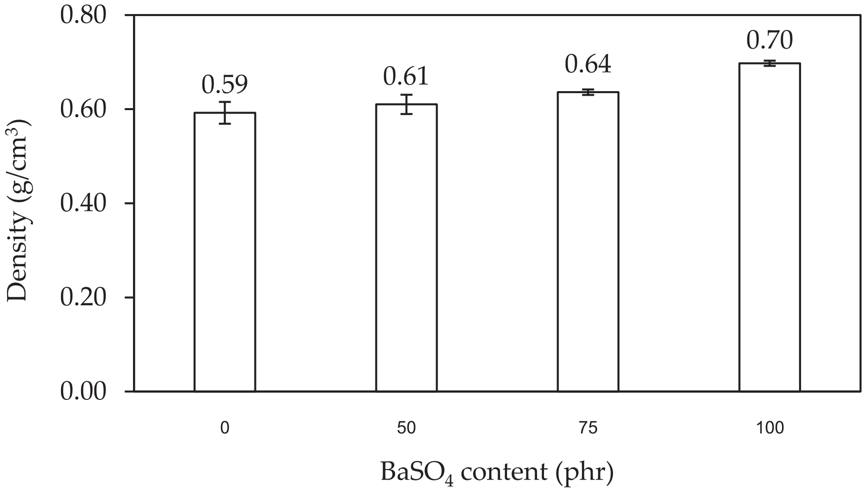

Figure 3. The densities of NR/$BaSO_4$ composites with varying contents of $BaSO_4$.

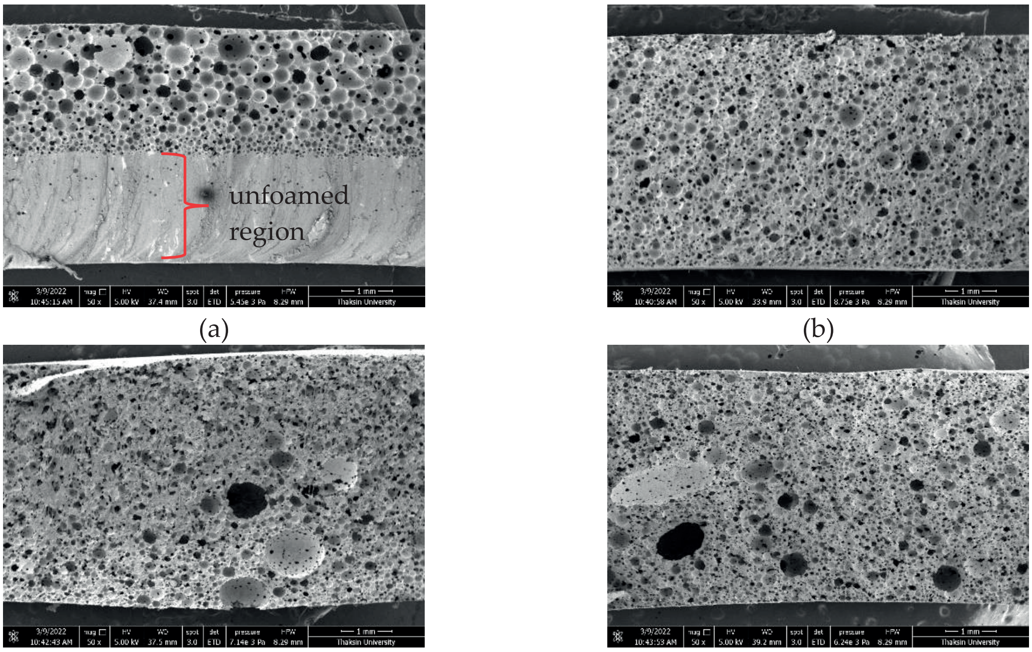

(a) (b) (c) (d)

Figure 4. Cross-sectional microstructures of NR/$BaSO_4$ composites with varying contents of $BaSO_4$ (a), 0 phr, (b) 50 phr, (c) 75 phr, and (d) 100 phr.

Figure 4. represents the influence of $BaSO_4$ on morphologies of NR/$BaSO_4$ composites. From cross-sectional microstructures, All samples showed small open-cell structures inside NR/$BaSO_4$ composites from cross-sectional microstructures. However, NR/$BaSO_4$ composites had non-uniform cell structures. The composites without $BaSO_4$ consisted of large foam cells on the top, the tiny foam cells in the middle, and the non-foamed region on the bottom (Figure 3 (a)). Due to foams transforming into solid-state foams slowly, it is easier to diffuse gas into the top of the sample, which leads to foam collapse and increased density on the bottom [14]. On the other hand, samples with increasing $BaSO_4$ contents showed increasing large voids since foams transformed to solid-state foams rapidly. Gas phases decrease tensile strength, elongation at break, and tear strength [3].

3.2 Mechanical properties

As shown in Figure 5, the tensile strength, elongation at break, and tear strength decreased with increasing $BaSO_4$ content. These were due to more $BaSO_4$ content being added to the composites, leading to an agglomeration of $BaSO_4$ particles and worse particle dispersion[16]. On the other hand, hardness (Shore A) increased with increasing $BaSO_4$ contents. The increases in hardness could have been due to the high rigidity of the $BaSO_4$ particles. This result was consistent with Lim-aroon et al. (2019) [16], which prepared X-ray and gamma-ray shielding from NR/Bi_2O_3 composites.

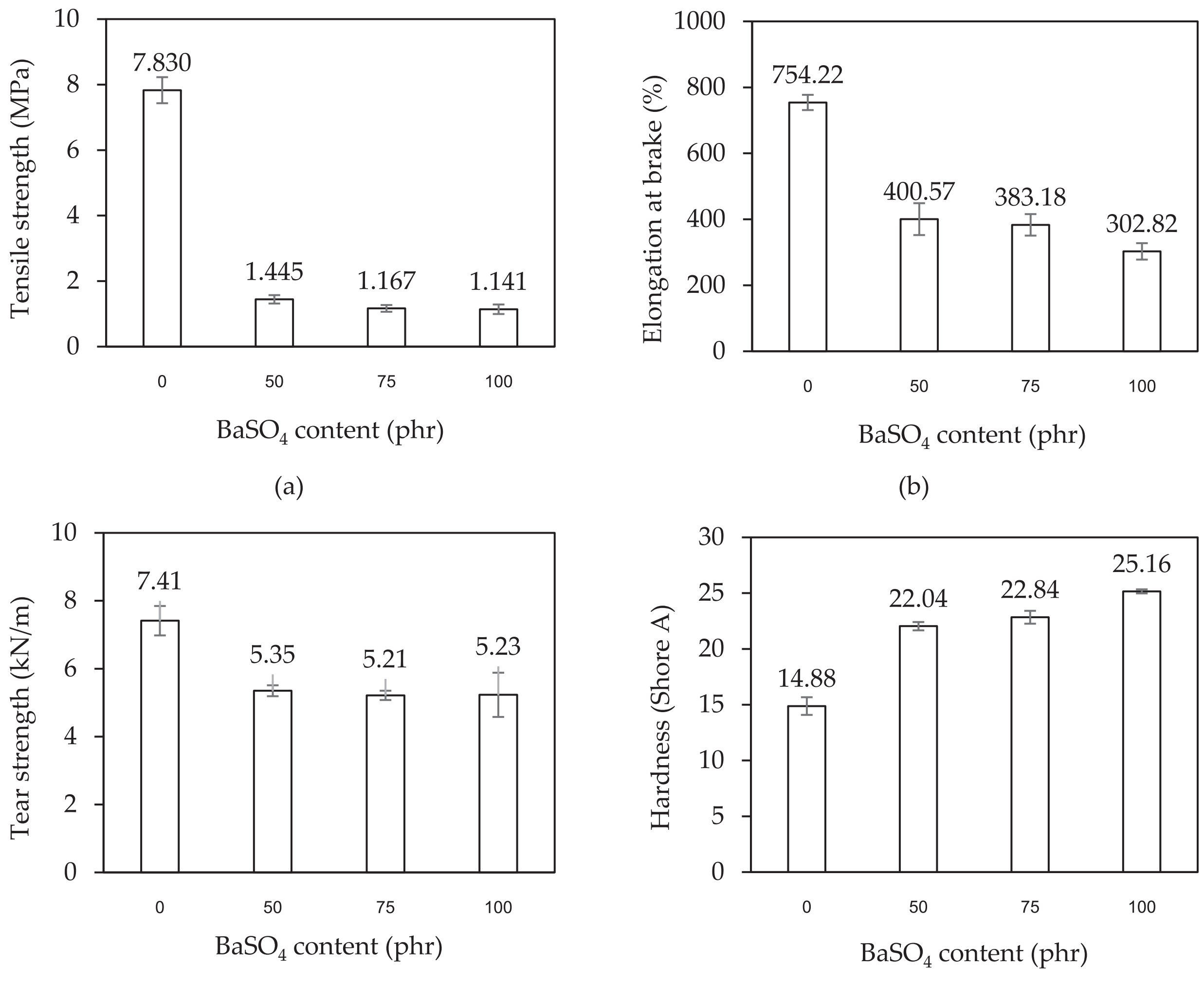

(a) (b)

(c) (d)

Figure 5. The mechanical properties of NR/$BaSO_4$ composites with varying contents of $BaSO_4$; (a) tensile strength, (b) elongation at break, (c) tear strength, and (d) hardness.

3.3 X-Ray shielding properties

Figure 6 shows the X-ray attenuation as a function of thickness for NR/$BaSO_4$ composites. It can be seen that the X-ray attenuation is higher compared to a pure NR. In addition, the X-ray attenuation increases with $BaSO_4$ content and thickness of samples due to the more remarkable ability of X-ray interaction and the impact of the photoelectric effect or Compton scattering with bismuth atoms in the material to attenuate and reduce X-ray energies and intensities [2]. For 2 cm thickness, the X-ray attenuation is highest at about 94% in 100 $BaSO_4$. From this result, it was possible to develop for actual use.

X-ray shielding properties of NR/$BaSO_4$ composites are shown in Table 2. The results showed that μ_l and μ_m increased, while HVL decreased with increasing $BaSO_4$ content. Causes may include the high Z number material ($BaSO_4$) [11], periodically distributed in the Na/$BaSO_4$ composites, which can act as an X-ray moderator resulting in μ_l improved HVL. At 100 phr of $BaSO_4$ content, the highest μ_l, μ_m, and the lowest HVL were 1.342 cm^{-1}, 1.923 cm^2/g, and 0.517 cm, respectively. These results confirm that increasing the contents of $BaSO_4$ could improve the radiation shielding properties of NR/$BaSO_4$ composites.

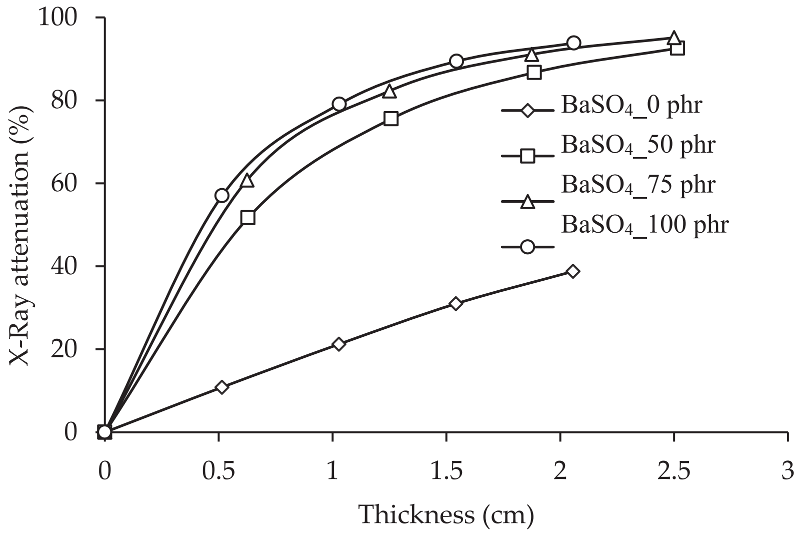

Figure 6. X-ray attenuation (%) of NR/$BaSO_4$ composites with varying contents of $BaSO_4$.

Table 2. The linear attenuation coefficient, mass attenuation coefficient and half-value layer of NR/$BaSO_4$ composites.

$BaSO_4$ content (phr)	**Linear attenuation coefficient; μ_l (cm^{-1})**	**Mass attenuation coefficient; μ_m (cm^2/g)**	**Half value layer;** HVL **(cm)**
0	0.241	0.406	2.880
50	1.092	1.79	0.635
75	1.203	1.891	0.576
100	1.342	1.923	0.517

4. Conclusions

This work developed flexibility, lead-free, X-ray shielding materials based on NR/$BaSO_4$ composites with the contents varied $BaSO_4$ from 0 to 50, 75, and 100 phr. The results showed that $BaSO_4$ worked effectively as active fillers to shield X-rays. The NR/$BaSO_4$ composites had a higher linear attenuation coefficient (μ_l) and mass attenuation coefficient (μ_m) with increasing $BaSO_4$, while the HVL was decreased. Furthermore, it was found that the X-ray attenuation property improved with increasing $BaSO_4$ content and material thickness. The results also indicated that the increasing $BaSO_4$ increased the density and hardness of NR/$BaSO_4$ composites.

5. Acknowledgements

This work was supported by National Higher Education, Science, Research and Innovation Policy Council, Thaksin University (Research project grant) Fiscal Year 2022.

Author Contributions: Conceptualization, S. K. and A. S.; designed the experiments, S. K. and A. S.; performed the experiments, S. K., A. S., F. T. and W. N.; analysis and investigation, S. K. and P. B.; writing—review and editing, S. K. and P. B.; All authors have read and agreed to the published version of the manuscript."

Funding: This research was funded by National Higher Education, Science, Research and Innovation Policy Council and Thaksin University (Research project grant) Fiscal Year 2022.

Conflicts of Interest: The authors declare no conflict of interest.

References

[1] Shepp, L. A.; Kruskal J. B. Computerized Tomography: The New Medical X-Ray Technology. *The American Mathematical Monthly*, 1978; *85*(6), 420-439.

[2] Toyen, D.; Saenboonruang, K. Comparative X-ray shielding properties of bismuth oxide/natural rubber composites using a Monte Carlo code of PHITS. *Materials Science and Engineering*, 2020, 773; 1-4.

[3] Onjun, O.; Buasuwan, N.; Rungseesumran, T.; Kamwang, N.; Channuie, J. Natural rubber block as gamma radiation shielding for medical applications. *Journal of Physics: Conference Series*, 2019, 1285; 1-8.

[4] Mirzaei, M.; Zarrebini, M.; Shirani, A.; Shanbeh, M.; Borhani, S. X-ray shielding by a novel garment woven with melt-spun monofilament weft yarn containing lead and tin particles. *Textile Research Journal*, 2019, *89*(1); 63–75.

[5] Khatib, A. M. E.; Doma, A. S.; Badawi, M. S. Rayan, A. E. A.; Aly, N. S.; Alzahrani, J. S.; Abbas, M. I. Conductive natural and waste rubbers composites-loaded with lead powder as environmental flexible gamma radiation shielding material. *Materials Research Express*, 2020; 7, 1-16.

[6] Kim, S.C.; Cho, S.H. Analysis of the Correlation between Shielding Material Blending Characteristics and Porosity for Radiation Shielding Films. *Applied Sciences*, 2019; *9*(9), 1-9.

[7] Poltabtim, W.; Wimolmala, E.; Saenboonruang, K. Properties of lead-free gamma-ray shielding materials from metal oxide/EPDM rubber composites. *Radiation Physics and Chemistry*, 2018; 153, 1–9.

[8] Poltabtim, W.; Wimolmala, E.; Markpin, T.; Sombatsompop, N.; Rosarpitak, V.; Saenboonruang, K. X-ray Shielding, Mechanical, Physical, and Water Absorption Properties of Wood/PVC Composites Containing Bismuth Oxide. *Polymers*, 2021; 13, 1-16.

[9] Toyen, D.; Rittirong, A.; Poltabtim, W.; Saenboonruang, K. Flexible, lead.free, gamma shielding materials based on natural rubber/metal oxide composites. *Iranian Polymer Journal*, 2018; 27, 33-41.

[10] Poltabtim, W.; Wimolmala, E.; Markpin, T.; Sombatsompop, N.; Rosarpitak, V.; Saenboonruang, K. X-ray Shielding, Mechanical, Physical, and Water Absorption Properties of Wood/PVC Composites Containing Bismuth Oxide. *Polymers*, 2021; 13, 1-16.

[11] Zhang, X.; Yang, M.; Zhang, X.; Wu, H.; Guo, S.; Wang, Y. Enhancing the neutron shielding ability of polyethylene composites with an alternating multi-layered structure. *Composites Science and Technology*, 2017; 150, 16-23.

[12] Cherkasov, V.; Yurkin, Y.; Avdinin, V.; Suntsov, D. Self-adhesion X-ray Shielding Composite Material of EPDM Rubber with Barite: Mechanical Properties. *Materiale Plastice*, 2020; *57*(1), 28-36.

[13] Akkurt, I.; Akyıldırım, H.; Mavi, B.; Kilincarslan, S.; Basyigit, C. Photon attenuation coefficients of concrete includes barite in different rate. *Annals of Nuclear Energy*, 2010; 37, 910–914.

[14] Sukkaneewat, B.; Utara, S. Ultrasonic-assisted Dunlop method for natural rubber latex foam production: Effects of irradiation time on morphology and physico-mechanical properties of the foam. *Ultrasonics Sonochemistry*, 2022; 82, 1-11.

[15] Phomrak, S.; Nimpaiboon, A.; Zhang Newby, B. Natural Rubber Latex Foam Reinforced with Microand Nanofibrillated Cellulose via Dunlop Method. *Polymer*, 2020; 12, 1-16.

[16] Lim-aroon, P.; Wimolmala, E.; Sombatsompop, N.; Saenboonruang, K. Manufacturing process and properties of lead-free natural rubber sponge for use in X-ray and gamma ray shielding applications. *IOP Conf. Series: Materials Science and Engineering*, 2019; 526, 1-4.

[17] Atichatkul. T.; Chanunpanich. N.; Pungkun V.; Suwanboon. C. X-ray Attenuation Coeffcient of PU/$BaSO_4$ Composite Sheet. *The Journal of KMUTNB*, 2017; *27*(1), 159-168.